J. exp. Biol. 154, 137–162 (1990)
Printed in Great Britain © The Company of Biologists Limited 1990

KINEMATICS OF THE TONGUE-BITE APPARATUS IN OSTEOGLOSSOMORPH FISHES

BY CHRISTOPHER P. J. SANFORD* AND GEORGE V. LAUDER

Department of Ecology and Evolutionary Biology, University of California, Irvine, CA 92717, USA

Accepted 6 June 1990

Summary

Osteoglossomorph fishes are characterized by the possession of three sets of jaws used during the capture, maceration and swallowing of prey. One of these jaw systems is a remarkable tongue-bite apparatus used during the intraoral crushing and shredding of prey. Kinematics of the tongue-bite apparatus were quantified, using 200 frames s^{-1} video and film records of feeding in three genera of osteoglossomorph fishes (*Osteoglossum*, *Pantodon* and *Notopterus*) to examine the biomechanics and function of this mechanical system. Two distinct chewing behaviors associated with the tongue-bite apparatus were identified: raking and open-mouth chewing. In all three species, raking behavior involves holding the prey firmly in the mandibular jaws while the teeth of the tongue-bite apparatus are moved into the prey. However, other aspects of raking behavior are significantly different among the species: for example, only *Notopterus* uses extensive posterior movement of the pectoral girdle to pull basihyal teeth through the prey. In both *Osteoglossum* and *Pantodon* there is little motion of the pectoral girdle, and neurocranial elevation plays the major mechanical role in prey reduction, but there are also kinematic differences between *Osteoglossum* and *Pantodon* during raking. The kinematics of open-mouth chewing behavior are also significantly different among the three species. Thus, osteoglossomorph fishes share a similar morphology of the tongue-bite apparatus derived from a common ancestor, but have acquired independent kinematic specializations associated with its use.

Introduction

One of the most remarkable biomechanical systems in ray-finned fishes is the tongue-bite apparatus of osteoglossomorphs, which possess three sets of jaws. Two of these, the mandibular jaw apparatus (MJA, which is the most anterior set of jaws) and the pharyngeal jaw apparatus (PJA, the most posterior set of jaws located in the pharynx), are present in all ray-finned fishes. Osteoglossomorph fishes, however, possess a third set of jaws, located between the MJA and PJA, which is often referred to as the tongue-bite apparatus (TBA, Lauder and Liem,

* Present address: Department of Biology, Emory University, Atlanta, GA 30322, USA.

Key words: Kinematics, feeding, fishes, high-speed video.

1983; Liem and Greenwood, 1981; Nelson, 1968; Sanford and Lauder, 1989). The tongue-bite apparatus consists of two main groups of teeth: teeth located on the base of the skull and palatal region, and teeth located on the hyobranchial apparatus (the 'tongue') at the floor of the mouth. These two groups of teeth bite against one another to shred and disable prey once they have been captured and before they have been swallowed (Sanford and Lauder, 1989).

The presence of a TBA is considered to be a derived feature for osteoglossomorph fishes (see Lauder and Liem, 1983), a clade composed of approximately 26 genera and 206 species. Other, distantly related, teleostean fishes have evolved a TBA independently (Lauder and Liem, 1983; Liem and Greenwood, 1981; Nelson, 1969*b*), but knowledge of the phylogenetic distribution of this feature in ray-finned fishes is still limited.

Although the unusual biomechanical properties of the TBA in osteoglossomorph fishes have attracted a number of morphological analyses (Bridge, 1895; Dagot and D'Aubenton, 1957; Greenwood, 1971; Kershaw, 1970, 1976; Nelson, 1968; Ridewood, 1905; Taverne, 1977, 1978), there are only two functional studies (Kershaw, 1976; Sanford and Lauder, 1989). Virtually nothing quantitative is known about the functional morphology of the TBA in osteoglossomorph fishes.

This paper has two main goals. First, to characterize quantitatively the kinematics of the TBA in three osteoglossomorph species: the arawana *Osteoglossum bicirrhosum* Vandelli, the African freshwater butterfly fish *Pantodon buchholzi* Peters and the clown knife fish *Notopterus chitala* Hamilton-Buchanan. This is done using an analysis of high-speed films and videos of chewing and prey manipulation. Secondly, we statistically compare the kinematics of the TBA in these three taxa to determine whether the overall similarity in the biomechanical pathways used during chewing is reflected in the kinematic patterns. Do the three species, which possess generally similar overall morphologies of the TBA, possess similar kinematic patterns?

Materials and methods

Morphological and cinematographic analyses were performed on three species of osteoglossomorph fishes: *Osteoglossum bicirrhosum*, *Pantodon buchholzi* and *Notopterus chitala*. Specimens were readily obtainable from commercial suppliers. All specimens were maintained in aquaria with filtered dechlorinated water at 27°C. The size range of the specimens studied depended on species and availability. *Osteoglossum bicirrhosum* ranged from 11.1 to 18.3 cm (mean standard length=14.5 cm; S.E.=2.10; N=3) and were juveniles. *Pantodon buchholzi* ranged from 5.7 to 6.7 cm (mean=6.1 cm; S.E.=0.31; N=3). *Notopterus chitala* ranged from 25.6 to 27.5 cm (mean=26.8 cm; S.E.=0.44; N=4). Individuals of *Pantodon* were adults whereas *Notopterus* specimens were large juveniles.

Anatomical observations were made on the feeding mechanism in these three taxa focusing on those structures associated with the TBA. Anatomical material examined consisted either of formalin-fixed specimens preserved in 70% ethyl

alcohol, or cleared and double-stained specimens (Dingerkus and Uhler, 1977) to display bone and cartilage. Representatives of all three species were examined. Both alcoholic and cleared and stained material were examined under a Zeiss IVB dissecting microscope with a *camera lucida* attachment which was used to produce diagrams of cranial osteology.

High-speed cinematography

Both high-speed film and high-speed video were used to study kinematics. High-speed films of *Osteoglossum* and *Notopterus* were obtained with Kodak 4X Reversal film in a Locam II 16 mm high-speed camera running at 200 frames s^{-1}. High-speed video of *Osteoglossum* and *Pantodon* feeding was obtained with a NAC HSV-400 high-speed video camera on standard VHS video tape with synchronized stroboscopic lights. Filming was conducted in black and white for higher resolution at 200 fields s^{-1}.

Both *Osteoglossum* and *Pantodon* are surface feeders and were thus fed live crickets at the surface of the water. *Notopterus* is a mid-water feeder and was fed live goldfish (*Carassius auratus*). All three taxa were trained to feed under lights in their own tanks with a background grid marked in centimeters. Only those chewing sequences occurring parallel to the film plane were analyzed, and we focused on obtaining film of intraoral chewing behavior involving the TBA.

Behaviors using the TBA were readily distinguishable from both initial prey capture and swallowing using the pharyngeal jaw apparatus. In video and film sequences involving the TBA, one end of the prey may be seen between the mandibular jaws, with the main body of the prey located within the buccal cavity. When prey are in this location the teeth of the TBA are directly applied to the dorsal and ventral margins of the prey. The action of the TBA on the prey is then inferred from measurement of the movements of the surrounding bony elements which may be clearly seen in a lateral view of the head.

Measurement of variables

Cranial movements of all three taxa were analyzed frame by frame using customized video and film digitizing software. From over 100 chewing cycles filmed for all three taxa 10–30 cycles were chosen from each taxon for detailed analysis. Exact sample sizes for each variable are given in Table 1. Sequences were chosen that most clearly showed the behaviors associated with the TBA, exhibited the least transverse motion relative to the film plane, and manifested the least obstruction of landmarks by the prey item. Approximately 3200 frames were digitized for this study. Landmarks were chosen on the head that could be reliably located in each frame and were stable anatomical points. Fig. 1 illustrates the measurements made from video fields of feeding in *Pantodon*.

From each frame analyzed in all species the following four variables were measured. Neurocranial elevation (NELE) was measured as the angle (in degrees) between two lines. One line was defined by two points along either the lateral line of the fish or the dorsal border of the body. The other line was defined by two

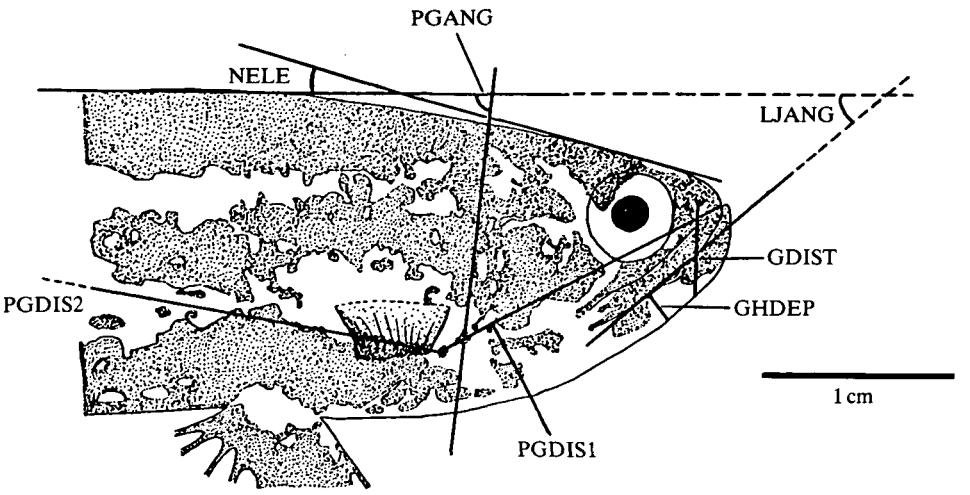

Fig. 1. Diagram of the head of the freshwater butterfly fish *Pantodon buchholzi* to show the kinematic variables measured from each field of high-speed video sequences of prey manipulation. The precise landmarks on the head differ slightly for the three genera used in this study. In addition, not all variables were measured for each species. A discussion of the measurements, interpretations and abbreviations of the variables is given in the Materials and methods.

points along the dorsal border of the neurocranium. This angle reflects the elevation of the neurocranium on the vertebral column as a result of contraction of the epaxial muscles: a decrease in the angle indicates neurocranial elevation.

Gape distance (GDIST) was defined as the distance (in cm) between the nostril or tip of the rostrum and the lower border of the dentary measured along a line perpendicular to the lateral line of the fish. Gape distance reflects change in gape which can result from both neurocranial elevation and lower jaw depression. An increase in GDIST indicates that the mouth is opening.

Pectoral girdle distance 1 (PGDIS1) is defined as the distance (in cm) from the nostril or tip of the rostrum, to an anterior point at the base of the pectoral fin. If, as in *Notopterus*, there are large excursions of the pectoral girdle during feeding, cranial elevation (i.e. change in NELE) will confound this measurement to some extent. Thus, care was taken to measure head movement simultaneously to allow us to correct for any bias in the measurement of PGDIS1.

Lower jaw angle (LJANG) is measured as the angle (in degrees) between two lines, one line being defined by two points along the lower border of the dentary and the other by two points along the lateral line or dorsal margin of the body. This angle reflects the mandibular depression with respect to the body axis and is independent of neurocranial movement. A decrease in lower jaw angle indicates lower jaw depression.

In both *Osteoglossum* and *Pantodon* two more variables were measured. Pectoral girdle distance 2 (PGDIS2) was defined as the distance (in cm) between a

fixed point towards the caudal region along the back, and an anterior point at the base of the pectoral fin. This measurement provides an indication of pectoral girdle motion not confounded by neurocranial elevation. Thus, changes in the position of the neurocranium have no effect on PGDIS2, and this variable was used to determine if there was any bias in the measurement of pectoral girdle distance 1. Geniohyoideus depression (GHDEP) was measured as the distance (in cm) from the lower border of the dentary to the maximal depression of the geniohyoideus muscle and associated connective tissue.

In addition, one further variable was measured in *Pantodon*. Pectoral girdle angle (PGANG) is defined as the angle (in degrees) between two lines. One line is defined by two points along the anterior border of the pectoral girdle, and the other by two points along the dorsal border of the fish. This angle reflects the rotation of the pectoral girdle, and as the angle increases the ventral tip of the pectoral girdle is rotating anteriorly.

Four kinematic variables could be compared directly across taxa (NELE, LJANG, PGDIS1, GDIST). To facilitate averaging variables across chewing cycles a 'zero time' was defined as the point that neurocranial angle (NELE) began to decrease rapidly indicating the onset of chewing behavior. This occurred in all chewing behaviors and was easily identified. For each species and each behavior a mean plot for each variable was constructed against time (e.g. Figs 4, 5 and 6). The mean was calculated for every 5 ms after time zero and plotted graphically with the standard error of the mean for that frame.

In addition to the mean plots of chewing behavior which represent average kinematic patterns, other measurements were made on individual kinematic plots for each variable. These additional variables permit statistical analysis within and among species. With zero time identified in all sequences, eight variables were measured from each feeding sequence using a Tektronix 4107 graphics terminal.

The amplitude of neurocranial elevation (AM-NELE, in degrees) was measured as the change in angle (in degrees) from time zero to maximal decrease in angle, and represents the maximal extent of neurocranial elevation. The amplitude of lower jaw angle (AM-LJANG, in degrees) was measured as the change in angle from time zero to either minimal or maximal lower jaw angle. The amplitude of pectoral girdle distance 1 (AM-PGDIS1, in centimeters) is defined as the change in distance from time zero to the maximal excursion of the pectoral girdle posteriorly. The amplitude of gape distance (AM-GDIST, in centimeters) is defined as the change in distance from time zero to either minimal or maximal gape distance (depending on the behavior).

In addition to these four amplitude variables, four variables reflecting the temporal course of movement were also measured. The time to maximal neurocranial elevation (TM-NELE) is defined as the time (in milliseconds) from the onset of neurocranial elevation (time zero) to minimal NELE, which represents maximal neurocranial elevation. The time to lower jaw angle (TM-LJANG) is defined as the time (in milliseconds) from time zero to the time of either maximal or minimal lower jaw angle. The time to maximal posterior

pectoral girdle motion (TM-PGDIS1) is defined as the time (in milliseconds) from time zero to the time of maximal excursion of the pectoral girdle posteriorly. The time to minimal or maximal gape distance (TM-GDIST) is defined as the time (in milliseconds) from time zero to either minimal or maximal gape distance.

Statistical analysis

Four types of statistical analyses were performed on the data. First, basic descriptive statistics were calculated and consisted of means, ranges and standard errors for each chewing behavior in each species as well as for each frame of the films digitized. Because the three species studied differ in body and head size, we also present the data for the two distance variables that may be subject to size effects as a percentage of head length.

Second, one-way analysis of variance with *a posteriori* contrasts was performed to determine if the mean values for kinematic data differed among the three species. Differences among species summarized in Table 2 are indicated by underlining linking those taxa that are *not* significantly different. A 0.05 level of significance was used.

Third, a principal components analysis (PCA) was performed (using the microcomputer statistics package SYSTAT) on the correlation matrix of the eight kinematic variables. This provided an indication of the major axes of multivariate variation in the kinematic variables measured. None of the variables used for the PCA was corrected for size *a priori*. Because a missing data value for any one variable will result in a missing value for all principal component scores, a second PCA was conducted in which missing values (18 out of 288 data points) were substituted with the mean value for that individual and species. These PCA results produced scatterplots that were very similar to the PCA which included the missing values, indicating that the mean-substituted PCA did not bias comparisons among species. Missing values result from an inability to see the landmarks necessary to make a kinematic measurement, and occurred mainly when the prey in the mouth obscured head landmarks. Thus, sample sizes given in Table 1 for the statistical comparisons may not correspond exactly to the number of points on the PCA plots.

Fourth, a multivariate analysis of variance (MANOVA) was conducted on the scores resulting from the principal components analysis to determine if the three species showed any multivariate differences in kinematic patterns.

Results

Morphology

We present only those aspects of cranial morphology that are important to understanding the function of the TBA, as purely morphological descriptions of osteoglossomorph cranial morphology have been presented elsewhere [D'Aubenton (1954), Bridge (1895), Dagot and D'Aubenton (1957), Greenwood (1970,

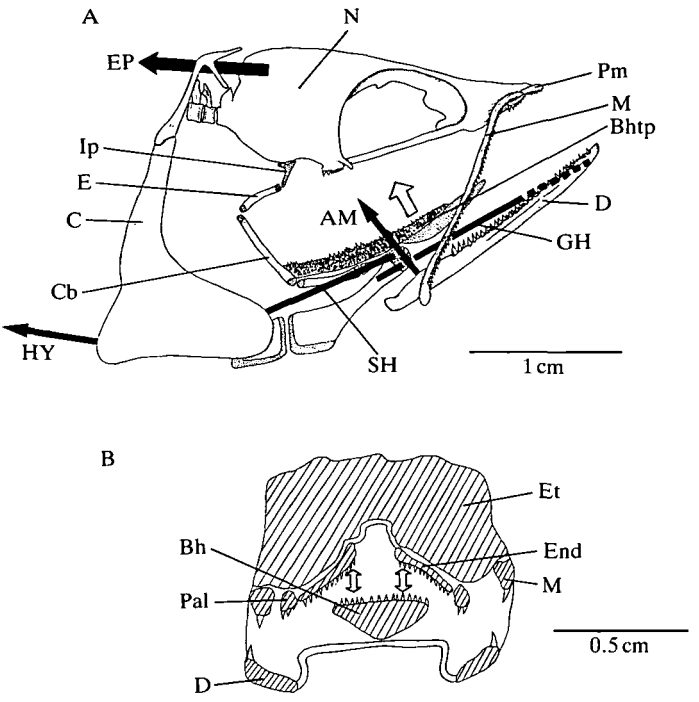

Fig. 2. Diagram of the cranial morphology of the osteoglossomorph fish *Osteoglossum bicirrhosum*. (A) Lateral view of the head and pectoral girdle, illustrating cranial osteology and myology as pertaining to the tongue-bite apparatus. The open arrow indicates the action of the basihyal teeth of the tongue-bite apparatus. Thick black lines indicate the lines of action of the major cranial muscles. (B) Cross-section of the ethmoid region of *Osteoglossum* showing the tongue-bite apparatus (indicated by open arrows) which consists ventrally of teeth on the basihyal and dorsally of opposing teeth on the ventral surface of the endopterygoid, parasphenoid and vomer. AM, adductor mandibulae muscle; Bh, basihyal; Bhtp, basihyal toothplate; C, cleithrum; Cb, ceratobranchial; D, dentary; E, epibranchial; Et, ethmoid cartilage; End, endopterygoid; EP, epaxial muscles; GH, geniohyoideus muscle; HY, hypaxial muscles; Ip, infrapharyngobranchial; M, maxilla; N, neurocranium; Pal, palatine bone; Pm, premaxilla; SH, sternohyoideus muscle.

1973), Kershaw (1970, 1976), Nelson (1968, 1969*a*,*b*), Omarkhan (1950), Ridewood (1904, 1905) and Taverne (1977, 1978)].

In all three taxa the mandibular jaw apparatus (MJA) consists of well-developed teeth around the anterodorsal rim of the dentary, and opposing teeth on the ventral margin of the premaxilla and maxilla (Fig. 2). The MJA produces the initial bite during prey capture. The pharyngeal jaw apparatus is similar to that of other primitive teleostean fishes and consists of one large ventral toothplate on each side and an opposing set of teeth consisting of small toothplates located on the ventral surface of infrapharyngobranchials 3 or 4 (Nelson, 1969*a*,*b*).

Intercalated between these two jaw systems is the TBA (Fig. 2A,B). In

Osteoglossum this consists of a set of teeth on the dorsal surface of the basihyal opposing a set of teeth on the ventral surface of the neurocranium and hyopalatine series (Fig. 2B). These teeth are distributed around the ventral surface of the vomer and the parasphenoid bone. In addition, there are teeth on the medial face of the endopterygoid and the ventral surface of the palatine bone. In *Pantodon* the TBA differs from that in *Osteoglossum* mainly in having larger teeth distributed on the ventral surface of the neurocranium and hyopalatine series. *Notopterus* possesses large teeth on the basihyal, and the dorsal opposing teeth are smaller than those in *Osteoglossum* and *Pantodon*.

Based on the morphology there appear to be two major functional components of the tongue bite: (1) direct apposition and crushing of prey between skull and hyobranchial teeth, and (2) shearing of prey as hyobranchial teeth slide past teeth on the palate (Fig. 2B). Both of these actions are anatomically possible in each of the three species, but the actual kinematics of the tongue bite depends on the sequence of muscle activity.

The cranial muscles of *Osteoglossum bicirrhosum* have been discussed by Greenwood (1971) and are only illustrated schematically here to aid in interpreting kinematic data (Fig. 2A). The muscles pertinent to the TBA are: the adductor mandibulae (AM), epaxial (EP), geniohyoideus (GH), hypaxial (HY) and sternohyoideus (SH) (Fig. 2A). The adductor mandibulae, the major jaw-closing muscle, is a large muscle originating on the lateral face of the hyobranchial series and inserting on the coronoid process of the dentary (Fig. 2A: AM). The epaxial muscles insert onto the posterodorsal region of the neurocranium and are the primary muscles involved in elevating the neurocranium (Fig. 2A: EP). The geniohyoideus muscle is a long slender muscle which runs from the lateral face of the anterohyal to the symphysis of the lower jaw (Fig. 2A: GH). This muscle is formed by fusion of the intermandibularis posterior and interhyoideus muscles (Lauder, 1980; Winterbottom, 1974) and acts to protract the hyobranchial apparatus.

The hypaxial muscles insert on the posterior and ventral margin of the cleithrum (Fig. 2A: HY) and are primarily involved in posterior rotation of the pectoral girdle. Finally, the sternohyoideus muscle (Fig. 2A: SH) originates from the anterior region of the cleithrum and inserts tendinously on the dorso- and ventrohyal bones of the hyoid arch. This muscle causes the hyobranchial series to move posteroventrally and also causes lower jaw depression *via* the mandibulo-hyoid ligament (Lauder, 1980).

In *Pantodon* the cranial muscles are similar to those in *Osteoglossum*. According to Greenwood (1971), *Pantodon* has separate posterior intermandibularis and interhyoideus muscles, although he indicates that they are not easily separable along their entire length. Our observations indicate that in *Pantodon* the fibers of these two muscle groups are indistinguishable and thus identify the muscle as a geniohyoideus. In contrast to both *Osteoglossum* and *Pantodon*, *Notopterus* has a separate posterior intermandibularis and interhyoideus muscle. In *Notopterus*, the posterior intermandibularis is a long muscle, functionally the same as the

geniohyoideus, extending from the symphysis of the lower jaw to the lateral face of the anterohyal (Sanford and Lauder, 1989).

Kinematics

Feeding in all three taxa can be divided into four distinct behaviors: (1) the initial strike at the prey, (2) raking of the prey within the mouth cavity, (3) open-mouth chewing and (4) swallowing. Both raking and open-mouth chewing involve the TBA and can be classified as intraoral prey-processing behaviors; thus, they are the focus of this study. Both of these behaviors occur after the prey has been captured. Raking behavior is named for the apparent effect of this behavior on the prey: kinematic analyses (presented below) indicate that the dorsal and ventral sets of teeth of the TBA are raked across the prey, causing a severe puncturing and shredding of the prey surface. Open-mouth chewing behavior is named for the slight jaw opening movements seen as the TBA is used on the prey located within the mouth cavity.

Raking behavior

Raking in *Notopterus* is only employed when feeding on larger prey items (Sanford and Lauder, 1989). In both *Osteoglossum* and *Pantodon* raking behavior is much more common even on smaller prey items, although visual observations indicate that the frequency of raking increases with increased size of prey. Raking occurs when the prey item is held fixed in the mandibular jaw apparatus and the TBA is used to immobilize and disarticulate the prey. Raking typically begins with a sudden and substantial increase in neurocranial elevation, as can be seen in the video fields of raking in *Osteoglossum* shown in Fig. 3.

Osteoglossum. In *Osteoglossum* raking behavior is characterized by a large decrease in neurocranial angle (Fig. 4; Table 1), indicating that the neurocranium is being elevated, undergoing average maximal excursions of 26° (Table 1). This excursion is significantly greater than that found in either *Notopterus* or *Pantodon* (Tables 1, 2). In *Osteoglossum* the average time to maximal neurocranial elevation is approximately 69 ms (Table 1). As the neurocranium moves dorsally there is little change in gape distance, the average maximal excursion being 0.17 cm, or 5% of the head length (Fig. 4; Table 1). This value is not significantly different from that for either *Pantodon* or *Notopterus* (Table 2). This small change in gape reflects the fact that the prey item is being held firmly in the mandibular jaws.

The lower jaw closes slightly during raking (i.e. gape distance decreases) and soon reaches a local minimum (Fig. 4: GDIST). Lower jaw angle increases concomitantly with neurocranial elevation to keep the prey fixed between the jaws. This is reflected in the kinematic profile of lower jaw angle in which the time to maximal amplitude is 70 ms (Table 1) while the time to maximal amplitude of neurocranial elevation is 69 ms. The average maximal amplitude of lower jaw angle is 29° and is significantly greater than that in *Pantodon* and *Notopterus* (Tables 1, 2). However, as there is little change in gape distance, the change in

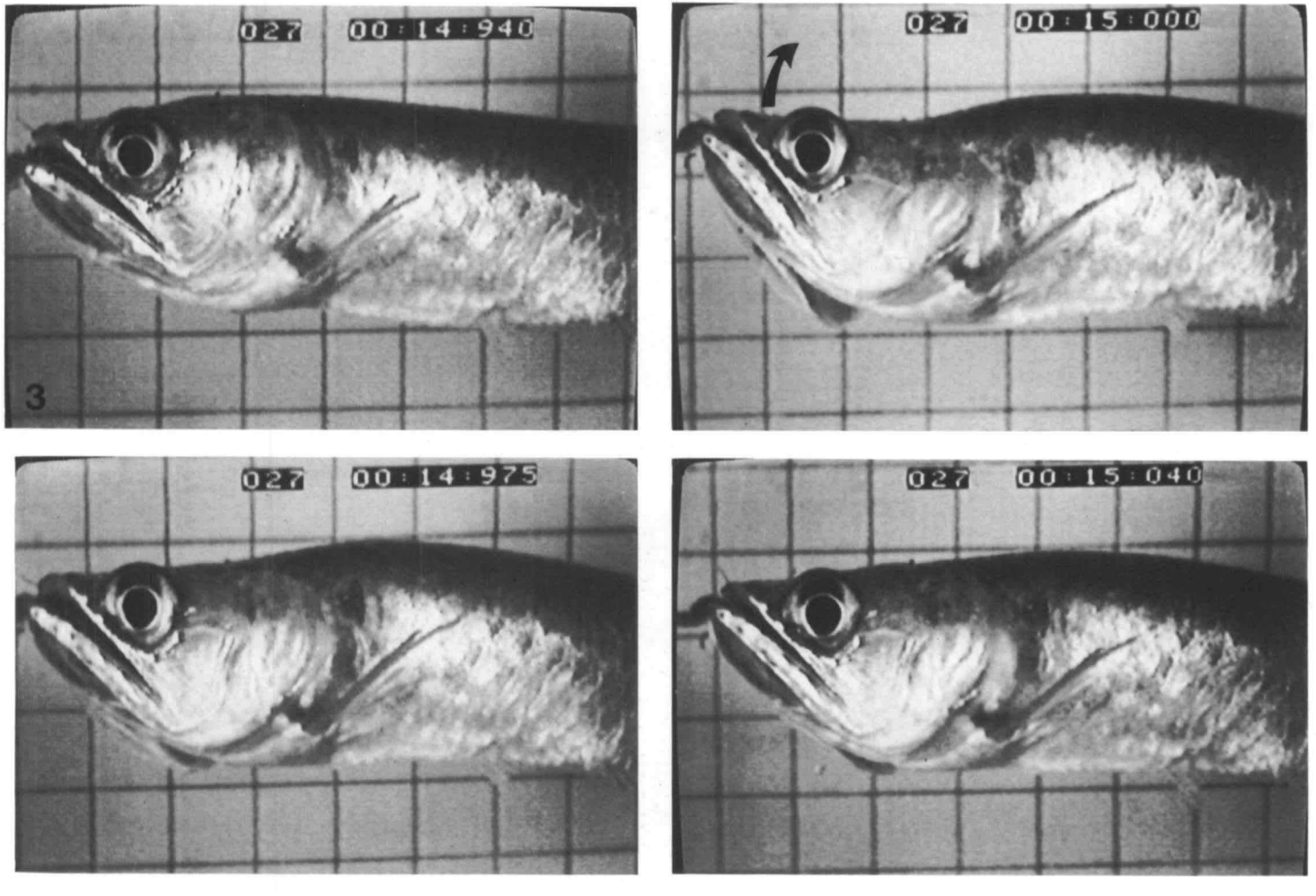

Fig. 3. Four fields from a high-speed video sequence of raking behavior in *Osteoglossum*. The numbers in the upper right-hand corner of each video field indicate the sequence number (027) and the time in milliseconds (from 14:940 at the start in the upper left field to 15:040 in the lower right field, a total duration of 100 ms). Note that the prey is held between the jaws in field 940 and that the head is strongly elevated in fields 14:975 and 15:000, as indicated by the arrow.

Table 1. *Summary of mean peak-to-peak and mean time-to-peak durations of four kinematic variables in* Notopterus, Osteoglossum *and* Pantodon

		AM-NELE (degrees)	AM-LJANG (degrees)	AM-PGDIS1 (cm)	AM-GAPE (cm)	TM-NELE (ms)	TM-LJANG (ms)	TM-PGDIS1 (ms)	TM-GAPE (ms)
Raking									
Osteoglossum	Mean	26.27	29.34	0.22(7%)	0.17(5%)	68.70	69.94	108.13	83.90
	S.E.	1.60	1.41	0.02	0.03	3.73	4.41	10.46	9.28
	N	15	15	14	15	15	15	14	12
Pantodon	Mean	15.74	18.72	0.21(12%)	0.10(6%)	48.01	28.79	51.02	24.95
	S.E.	1.76	1.81	0.05	0.03	9.59	3.32	10.06	4.75
	N	13	13	10	12	13	13	10	11
Notopterus	Mean	17.52	10.00	1.72(25%)	0.2.1(3%)	74.40	64.44	69.10	57.39
	S.E.	1.58	1.28	0.07	0.06	2.25	6.08	5.94	9.52
	N	8	8	8	6	*8*	*8*	8	6
Open-mouth chewing									
Osteoglossum	Mean	17.51	11.47	0.29(9%)	0.90(28%)	49.57	32.40	41.56	37.30
	S.E.	1.21	2.06	0.02	0.08	8.08	3.97	8.31	5.62
	N	15	15	15	15	15	15	15	15
Pantodon	Mean	4.99	7.74	0.13(8%)	0.53(31%)	55.73	30.55	44.98	50.14
	S.E.	0.85	0.63	0.03	0.07	11.57	4.14	8.62	6.79
	N	11	11	11	11	11	11	11	11
Notopterus	Mean	6.93	16.14	0.47(7%)	0.87(13%)	70.20	54.83	61.52	58.97
	S.E.	0.66	0.92	0.10	0.07	6.75	6.08	6.74	4.75
	N	11	11	11	11	11	11	11	11

Numbers in parentheses represent the distances measured as a percentage of the head length.

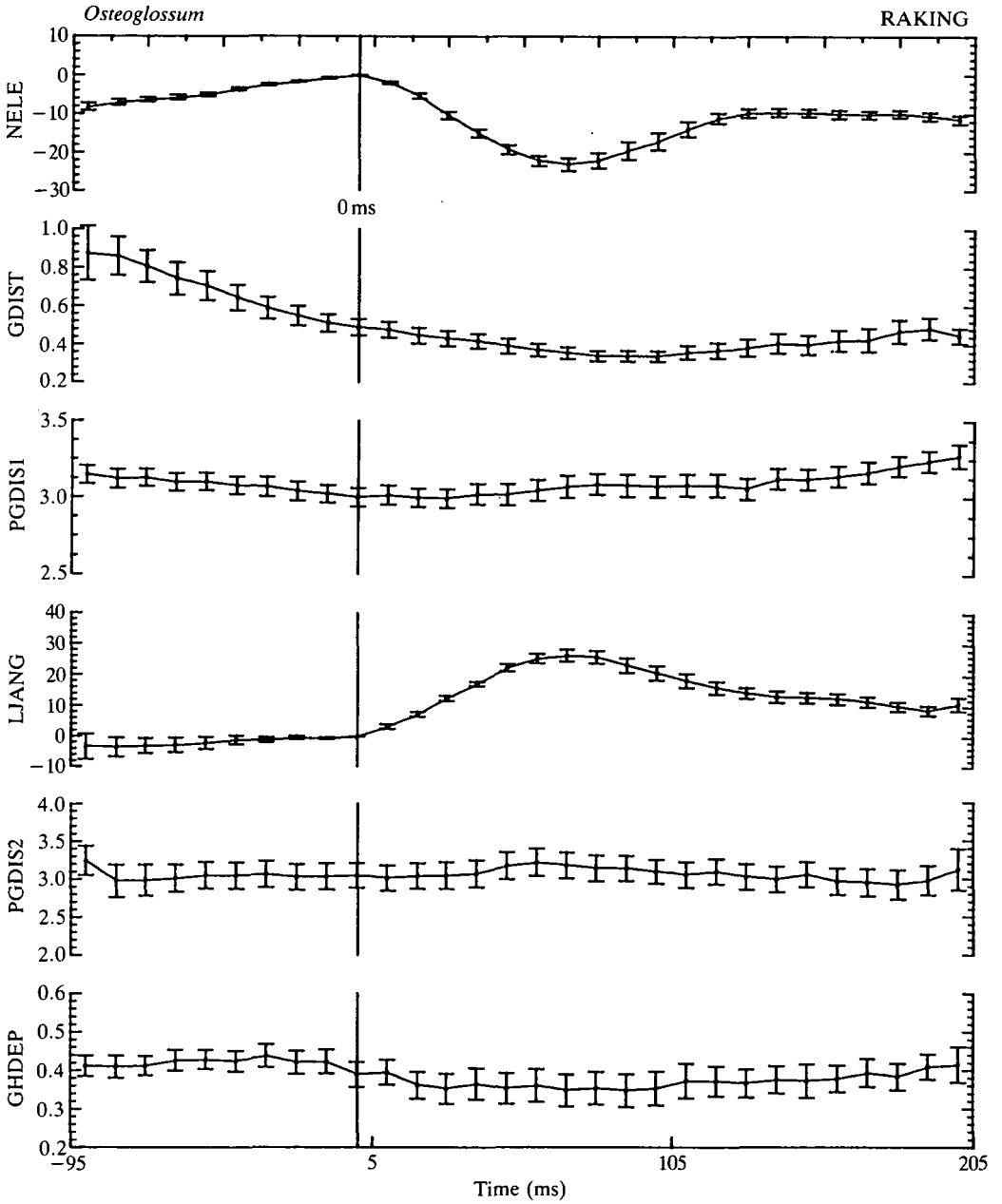

Fig. 4

lower jaw angle appears to be primarily the result of tracking neurocranial elevation.

During the main portion of the rake the pectoral girdle changes little in position, having a maximal posterior excursion of 0.22 cm, or 7 % of the head length (Fig. 4:

Fig. 4. Kinematic summary of raking behavior in *Osteoglossum bicirrhosum*. Variables shown are mean neurocranial elevation (NELE, in degrees), gape distance (GDIST, in cm), pectoral girdle distance 1 (PGDIS1, in cm), lower jaw angle (LJANG, in degrees), pectoral girdle distance 2 (PGDIS2, in cm) and geniohyoideus depression (GHDEP, in cm). These variables are plotted as a function of time in milliseconds, with the standard error for the mean in each 5 ms time interval indicated by a vertical bar. Each mean value is the average of between 8 and 15 points. Time zero (labelled 0 ms, and marked by the vertical lines) indicates the onset of raking, which is defined by a sharp decrease in the angle NELE, indicating an increase in neurocranial elevation. Note that as the lower jaw angle increases the mandible is being raised.

PGDIS1). As one point used to measure PGDIS1 is a fixed location on the rostrum, PGDIS1 might be confounded by dorsal rotation of the neurocranium during the power stroke. Therefore, a second variable was measured from the pectoral girdle to a fixed point well behind the pectoral fin, along the flank of the body (PGDIS2). The kinematic profile of PGDIS2 shows almost no change in value during the power stroke (Fig. 4), indicating that the angular rotation of the neurocranium has little effect on the value of PGDIS1. Finally, little change in the depression of the geniohyoideus was observed during raking (Fig. 4: GHDEP).

Pantodon. The onset of raking is identified by a sharp decrease in neurocranial angle (Fig. 5: NELE), indicating neurocranial elevation. The maximal excursion seen in *Pantodon* is significantly less than that found in *Osteoglossum* but not significantly different from that in *Notopterus* (Tables 1, 2). The average maximal excursion of the neurocranium is significantly less than that in *Osteoglossum*, but not significantly different from that in *Notopterus* (Tables 1, 2). Time-to-peak neurocranial elevation is significantly less than that in either *Osteoglossum* or *Notopterus* (Tables 1, 2).

A characteristic feature of raking behavior is that gape distance changes little, decreasing slightly as the head is lifted (Fig. 5: GDIST; Table 1: AM-GAPE). This decrease in gape is not significantly different from that in either of the other two taxa (Table 2). Lower jaw angle increases concomitantly with the dorsal rotation of the neurocranium (Fig. 5: LJANG). It is interesting to note that in *Pantodon* the lower jaw releases its hold on the prey prior to maximal neurocranial elevation. This is illustrated in Table 1, where time-to-peak lower jaw angle is 29 ms, while

Table 2. *Summary of ANOVA results for the variables used for Table 1*

	AM-NELE (degrees)	AM-LJANG (degrees)	AM-PGDIS1* (cm)	AM-GAPE* (cm)	TM-NELE (ms)	TM-LJANG (ms)	TM-PGDIS1 (ms)	TM-GAPE (ms)
Raking	N O P	N O P	N O P	N O P	N O P	N O P	N O P	N O P
Open-mouth chewing	N O P	N O P	N O P	N O P	N O P	N O P	N O P	N O P

*These analyses were performed on measurements expressed as a percentage of head length.
N, *Notopterus*; O, *Osteoglossum*; P, *Pantodon*.
Underlining indicates taxa that are *not* significantly different from one another.

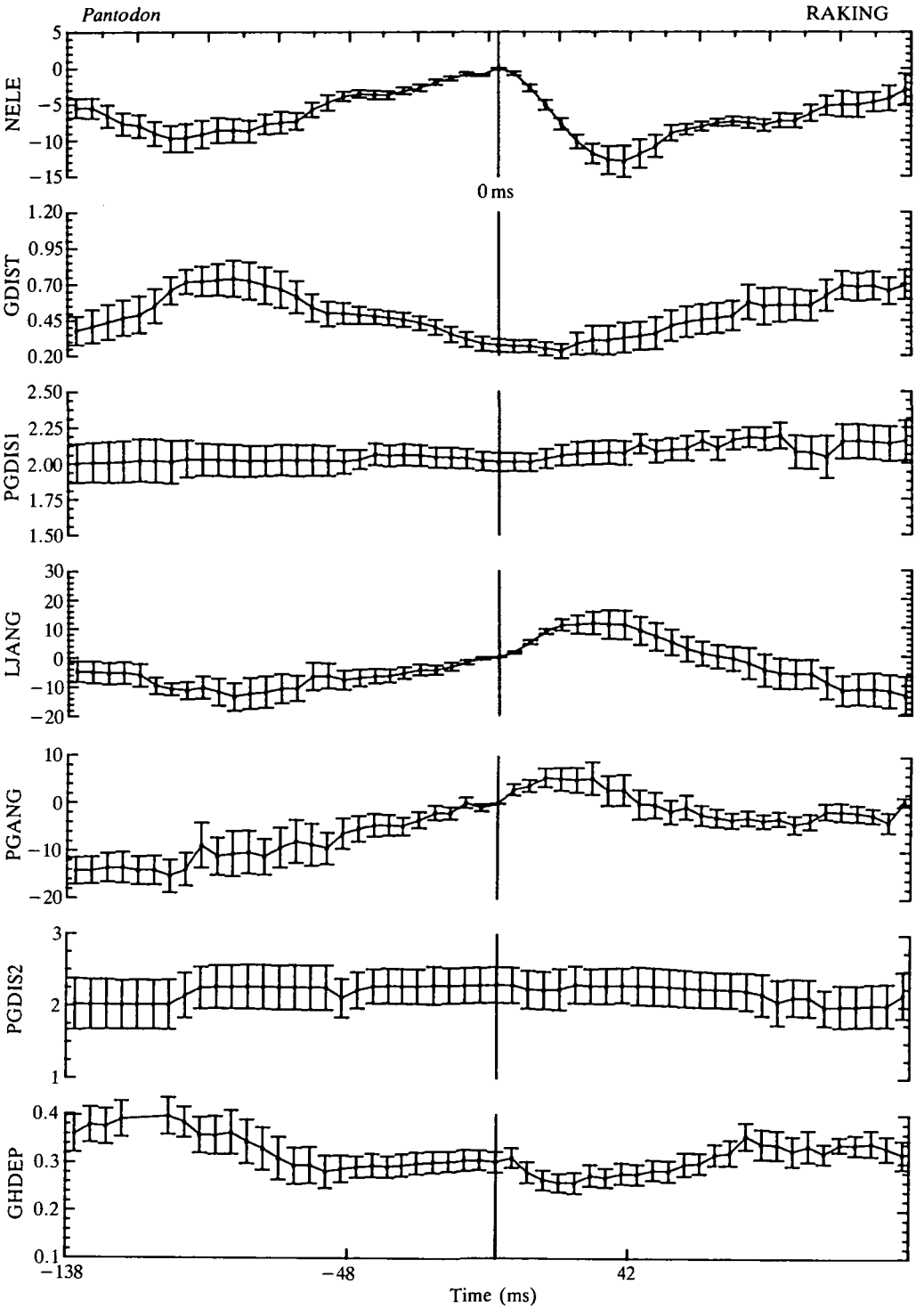
Pantodon
RAKING
NELE
5
0
−5
−10
−15
0 ms
GDIST
1.20
0.95
0.70
0.45
0.20
PGDIS1
2.50
2.25
2.00
1.75
1.50
LJANG
30
20
10
0
−10
−20
PGANG
10
0
−10
−20
PGDIS2
3
2
1
GHDEP
0.4
0.3
0.2
0.1
−138
−48
42
Time (ms)

Fig. 5

Fig. 5. Kinematic summary of raking behavior in *Pantodon buchholzi*. Variables shown are mean neurocranial elevation (NELE, in degrees), gape distance (GDIST, in cm), pectoral girdle distance 1 (PGDIS1, in cm), lower jaw angle (LJANG, in degrees), pectoral girdle angle (PGANG, in degrees), pectoral girdle distance 2 (PGDIS2, in cm) and geniohyoideus depression (GHDEP, in cm). These variables are plotted as a function of time in milliseconds, with conventions as in Fig. 4. Note that an increase in the pectoral girdle angle indicates rotation of the pectoral girdle in a counterclockwise direction (i.e. the ventral point of the pectoral girdle moves anteriorly).

time to maximal neurocranial elevation is 48 ms. This subtle release of pressure on the prey item is also indicated by the slight increase in gape distance before maximal neurocranial elevation (Fig. 5).

Another salient feature of raking in *Pantodon* is the relative lack of anteroposterior motion in the pectoral girdle. Neither pectoral girdle distance 1 nor 2 change dramatically (Fig. 5), with a maximal excursion of 0.21 cm or 12 % of the head length (Table 1). This change is significantly greater than that in *Osteoglossum*, but significantly smaller than that in *Notopterus* (Table 2). The increase in pectoral girdle angle (Fig. 5: PGANG) represents a counterclockwise rotation of the pectoral girdle such that the ventral tip of the pectoral girdle moves anteriorly. The amount of the rotation, however, is small (5–8°) and has little effect on pectoral girdle distance measures.

Notopterus. During raking, gape distance in *Notopterus* changes little (Fig. 6), undergoing a maximal excursion of 0.21 cm or 3 % of the head length (Table 1). In common with *Pantodon*, the gape distance at the onset of raking decreases slightly then increases, indicating that the initial closure of the lower jaw is followed by a slight release of pressure on the prey item.

A distinctive feature of raking in *Notopterus* is the massive excursion of the pectoral girdle, which on average amounts to 1.72 cm or 25 % of the head length (Fig. 6 and Table 1: PGDIS1 and AM-PGDIS1). As the pectoral girdle moves posteriorly, the neurocranium is elevated with a concomitant increase of the lower jaw angle (Fig. 6). The amount of neurocranial elevation is not significantly different from that in *Pantodon*, but is significantly less than that in *Osteoglossum* (Tables 1, 2).

Open-mouth chewing behavior

Open-mouth chewing is the second distinctive intraoral prey-processing behavior exhibited by these three taxa. The prey is held within the oral cavity and the TBA is used to chew on the prey. Open-mouth chewing can occur after or prior to raking, and the two behaviors often occur in cycles. Open-mouth chewing is a common behavior in all three taxa after a prey item has been captured.

Osteoglossum. In *Osteoglossum* open-mouth chewing occurs much more rapidly than raking. Indeed, for *Osteoglossum* all timing variables except neurocranial elevation are approximately half those of raking (Table 1). As with raking, the onset of open-mouth chewing in *Osteoglossum* is characterized by an

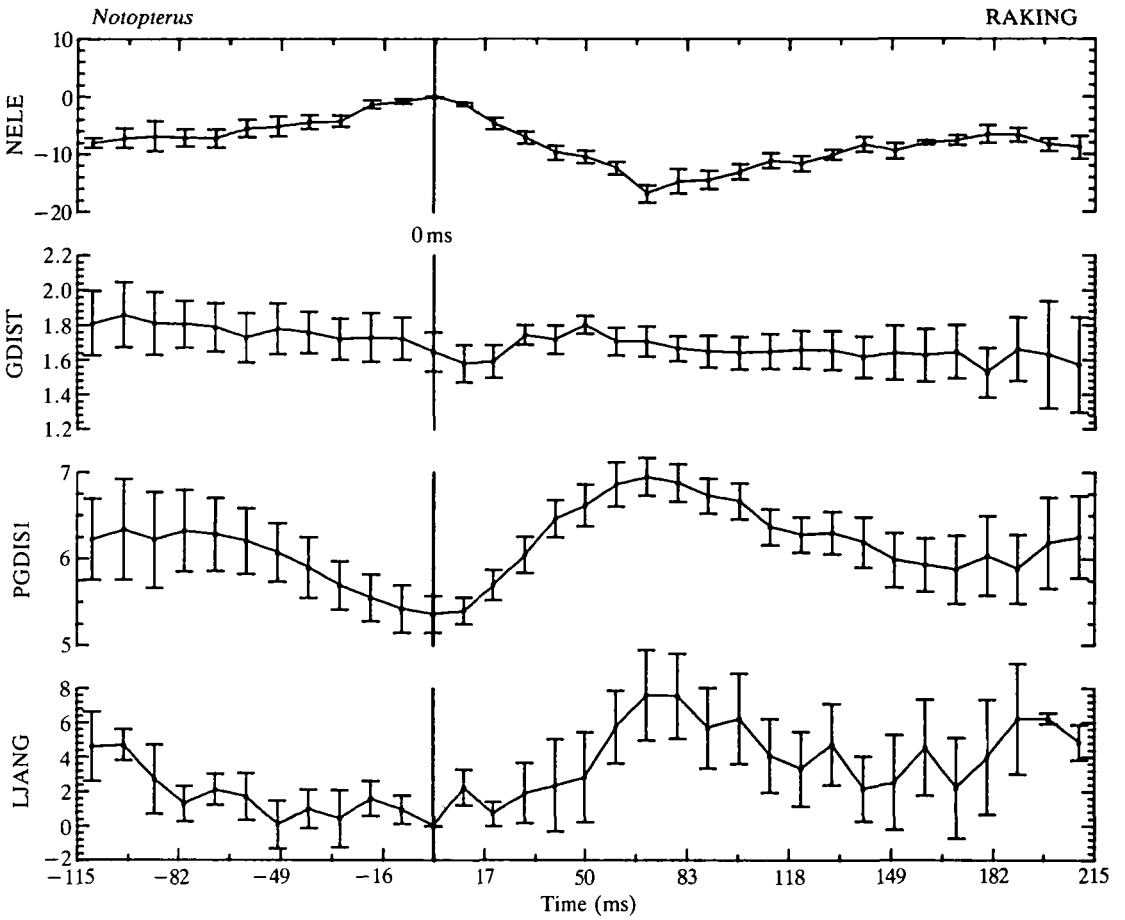

Fig. 6. Kinematic summary of raking behavior in *Notopterus chitala*. Variables shown are mean neurocranial elevation (NELE, in degrees), gape distance (GDIST, in cm), pectoral girdle distance 1 (PGDIS1, in cm) and lower jaw angle (LJANG, in degrees). Conventions as in Figs 4 and 5.

acute increase in neurocranial elevation, indicated by a sharp decrease in the cranial angle (Fig. 7: NELE), on average 17.5° (Table 1). This value is significantly greater than that in either *Pantodon* or *Notopterus* (Tables 1, 2).

At the beginning of neurocranial elevation there is a decrease in lower jaw angle followed by a slow increase (Fig. 7). This indicates that lower jaw depression is followed by raising of the lower jaw. Although lower jaw angle undergoes a greater excursion in raking (Table 1), the initial change in angle during open-mouth chewing is negative, indicating lower jaw depression.

During the initial stages of open-mouth chewing, depression of the lower jaw causes a change in both gape distance and lower jaw angle. The average gape distance increases to a maximal value of 0.90 cm or 28% of the head length

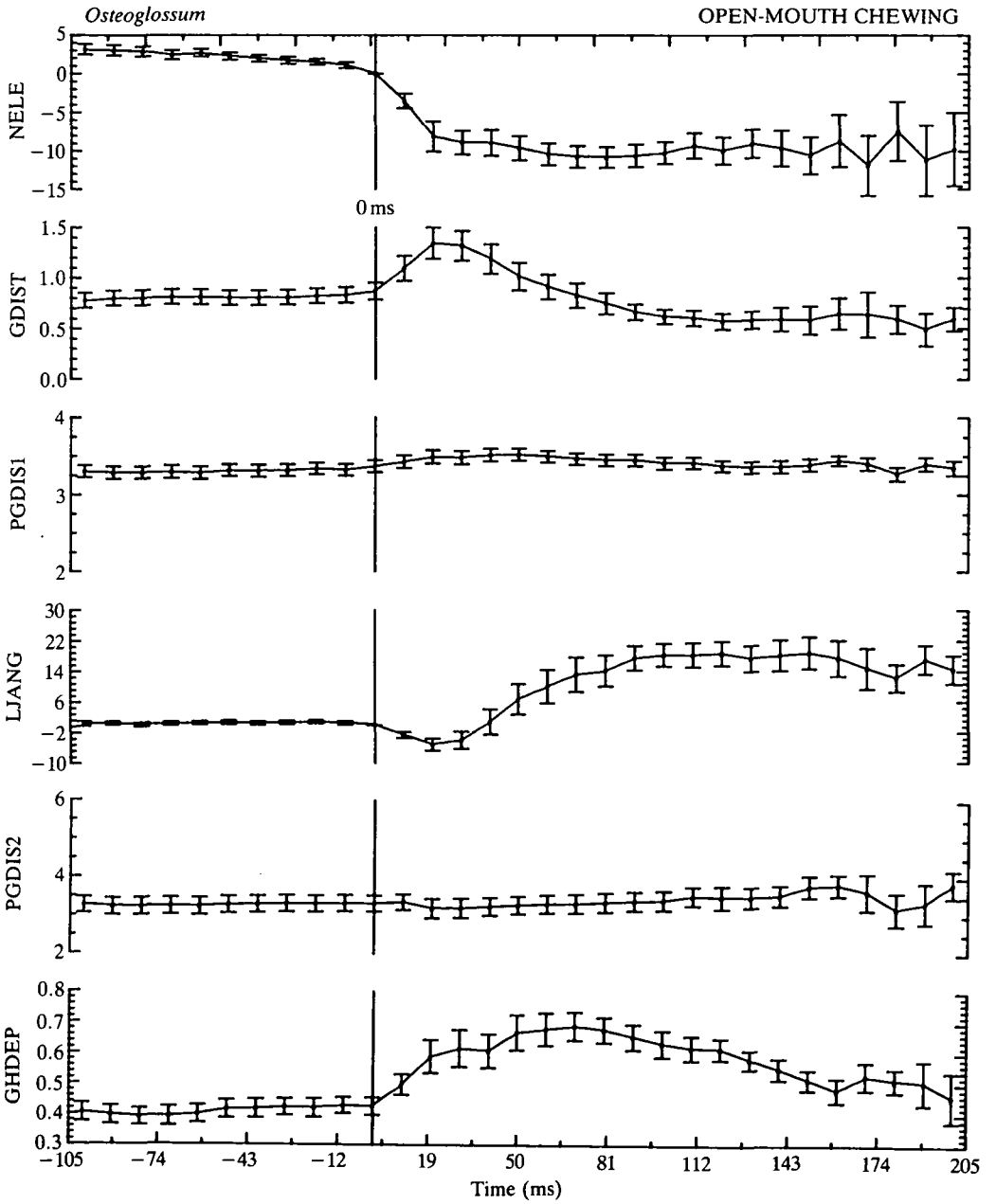

Fig. 7. Kinematic summary of open-mouth chewing in *Osteoglossum bicirrhosum*. Variables shown are mean neurocranial elevation (NELE, in degrees), gape distance (GDIST, in cm), pectoral girdle distance 1 (PGDIS1, in cm), lower jaw angle (LJANG, in degrees), pectoral girdle distance 2 (PGDIS2, in cm) and geniohyoideus depression (GHDEP, in cm). These variables are plotted as a function of time in milliseconds. Time zero indicates the onset of open-mouth chewing, which is defined by a sharp decrease in the angle NELE, indicating an increase in neurocranial elevation. Other conventions as in Figs 4 and 5.

(Table 1). It is important to note that the large change in gape distance is attributable to a change in both neurocranial elevation and lower jaw depression.

During open-mouth chewing there is almost no anteroposterior motion of the pectoral girdle (Fig. 7: PGDIS1 and PGDIS2). The average maximal excursion of the pectoral girdle is 0.29 cm or 9 % of the head length (Table 1), and this value is not significantly different from that in either *Pantodon* or *Notopterus* (Table 2). Geniohyoideus depression increases to a maximal value as the neurocranium elevates and then slowly returns to its original value (Fig. 7). This indicates that the geniohyoideus region of the buccal cavity is being pushed out as a result of the inflow of either water or the prey item as the mouth is being closed.

Pantodon. Open-mouth chewing begins with a decrease in neurocranial angle which indicates neurocranial elevation (Fig. 8: NELE). Peak neurocranial angle is significantly less than that in *Osteoglossum* (Table 2), having an average maximal excursion of 5° (Table 1). At the time of neurocranial elevation, the mouth opens, indicated by both a decrease in lower jaw angle and a concomitant increase in gape distance (Fig. 8). The decrease in lower jaw angle is intermediate between those of the other taxa, not significantly different from that in *Osteoglossum* but small in comparison to *Notopterus* (Tables 1, 2). Gape distance increases slowly (Fig. 8) but has a relatively high amplitude, averaging 0.53 cm or 31 % of the head length (Table 1). This value is not significantly different from that in *Osteoglossum* but is considerably more than that in *Notopterus* (Table 2).

As with *Osteoglossum* the pectoral girdle in *Pantodon* does not change position dramatically, undergoing an average shift of 0.13 cm or 8 % of the head length (Fig. 8: PGDIS1 and PGDIS2; Table 1: PGDIS1). During open-mouth chewing the pectoral girdle angle changes erratically and shows considerable variation with no general pattern of movement. In addition, geniohyoideus depression shows no consistent pattern of change.

Notopterus. During open-mouth chewing the neurocranium undergoes only a small change in angle (Fig. 9), amounting to approximately 7° on average. This mean value for maximal neurocranial elevation during open-mouth chewing is significantly smaller than that in *Osteoglossum*, but not significantly different from that in *Pantodon* (Tables 1, 2: AM-NELE).

Mean gape distance undergoes excursions of almost 0.87 cm or 13 % of the head length. This change in gape distance is, however, significantly smaller than that in either *Osteoglossum* or *Pantodon* (Table 2). As there is only a small change in neurocranial angle, the increase in gape distance must be attributable to lower jaw depression. Depression of the lower jaw in *Notopterus* is indicated by a rapid decrease in lower jaw angle (Fig. 9). The average maximal decrease in lower jaw

Fig. 8. Kinematic summary of open-mouth chewing in *Pantodon buchholzi*. Variables shown are mean neurocranial elevation (NELE, in degrees), gape distance (GDIST, in cm), pectoral girdle distance 1 (PGDIS1, in cm), lower jaw angle (LJANG, in degrees), pectoral girdle angle (PGANG, in degrees), pectoral girdle distance 2 (PGDIS2, in cm) and geniohyoideus depression (GHDEP, in cm). These variables are plotted as a function of time in milliseconds. Conventions as in Figs 4 and 5.

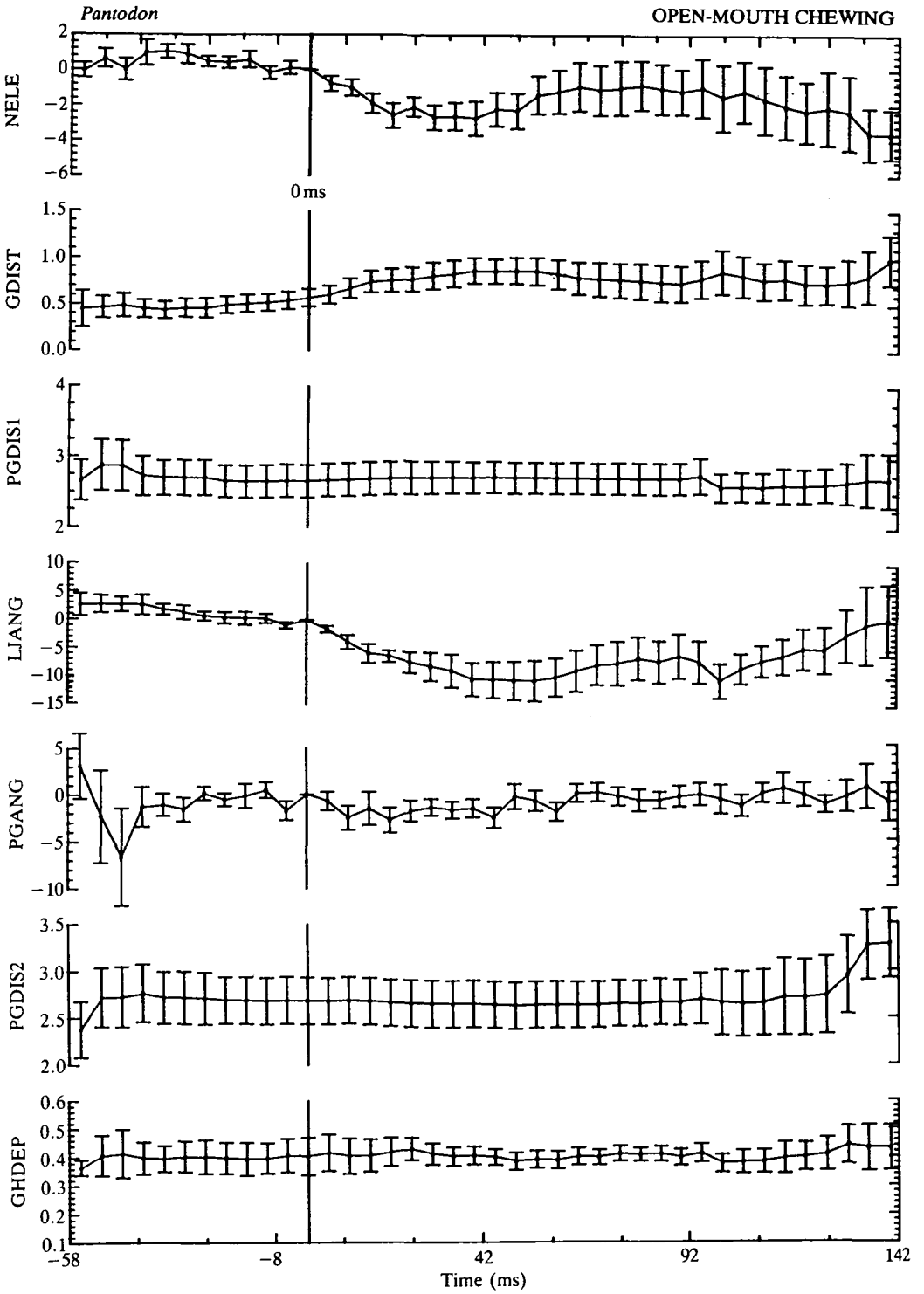
Pantodon
OPEN-MOUTH CHEWING
NELE
2
0
−2
−4
−6
0 ms
GDIST
1.5
1.0
0.5
0.0
PGDIS1
4
3
2
LJANG
10
5
0
−5
−10
−15
PGANG
5
0
−5
−10
PGDIS2
3.5
3.0
2.5
2.0
GHDEP
0.6
0.5
0.4
0.3
0.2
0.1
−58
−8
42
92
142
Time (ms)

Fig. 8

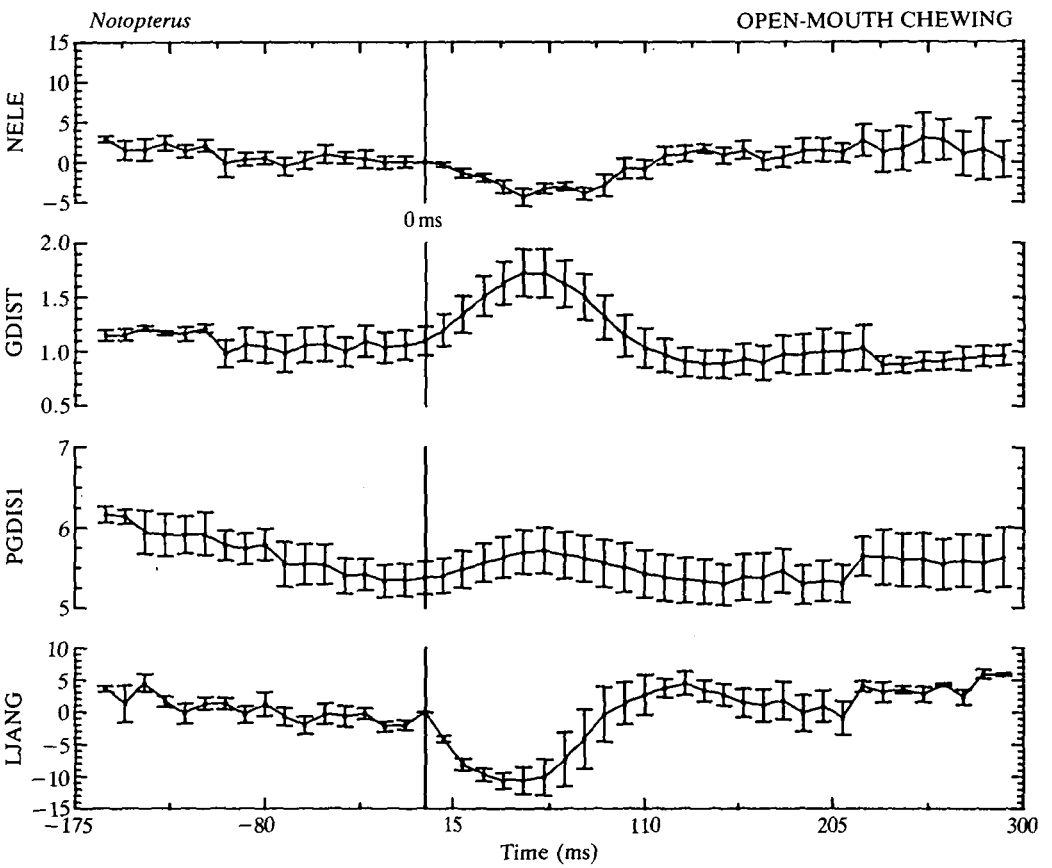

Fig. 9. Kinematic summary of open-mouth chewing in *Notopterus chitala*. Variables shown are mean neurocranial elevation (NELE, in degrees), gape distance (GDIST, in cm), pectoral girdle distance 1 (PGDIS1, in cm) and lower jaw angle (LJANG, in degrees). Conventions as in Figs 4 and 5.

angle is significantly greater than that in either *Osteoglossum* or *Pantodon* (Tables 1, 2).

During open-mouth chewing, concomitant with both lower jaw depression and neurocranial elevation, there is a slight increase in pectoral girdle distance (Fig. 9: PGDIS1). On average there is an increase in pectoral girdle distance of 0.47 cm or 7 % of the head length (Table 1). This value is not significantly different from that in either *Osteoglossum* or *Pantodon* (Table 2).

Principal component analysis

Patterns of kinematic variation during both raking and open-mouth chewing are summarized in a principal components analysis illustrated in Figs 10 and 11. The loadings of eight variables are presented in Table 3. In raking, components 1 and 2 account for 42.6 % and 24.8 %, respectively, of the variation in the data set and,

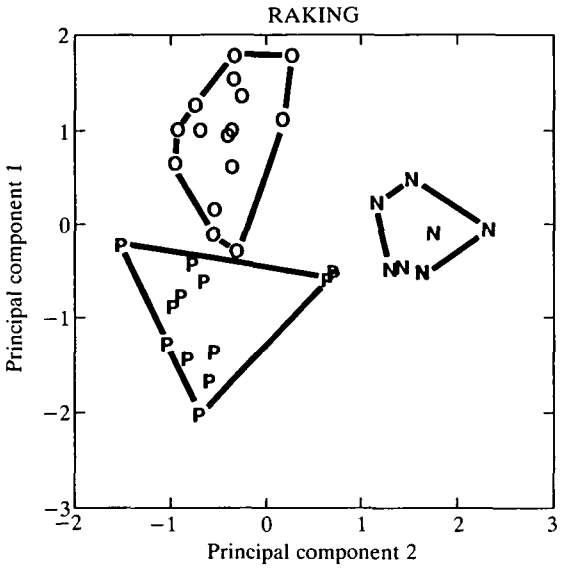

Fig. 10. Principal components (PC) analysis of raking behavior for eight kinematic variables plotted as PC1 *versus* PC2. Principal components 1–4 account for the following percentages of the overall variance in the data set: PC1, 42.6%; PC2, 24.8%; PC3, 11.4%; PC4, 7.9%. Each feeding is represented by one symbol for each species (O, *Osteoglossum*; P, *Pantodon*; N, *Notopterus*). Note that each osteoglossomorph species has a distinct kinematic pattern during raking (the polygons enclosing the feedings in each species do not overlap). The centroids for the species polygons are significantly different from each other (MANOVA $P<0.001$).

when plotted, clearly show that raking behavior is different in multivariate kinematic space in all three taxa (Fig. 10). High scores on principal component 1 reflect a greater extent of neurocranial elevation and lower jaw angle and a greater time-to-peak neurocranial elevation, lower jaw angle, pectoral girdle distance and gape (Fig. 10, Table 3). High scores on principal component 2 reflect increased motion in the pectoral girdle and gape, decreased motion in the angle of the lower jaw and increased time-to-peak neurocranial elevation (Fig. 10, Table 3).

In open-mouth chewing the principal component plots indicate that there is a great deal of overlap between taxa in multivariate kinematic space (Fig. 11). Principal component 1 does not separate the three taxa. High scores on principal component 2 reflect increased movement of the lower jaw (both lower jaw angle and gape distance) and increased motion of the pectoral girdle (Table 3), attributes in which *Notopterus* differs from *Pantodon*. High scores on principal component 3 indicate an increased level of motion in the neurocranium (AM-NELE) and decreased level of change in the lower jaw angle (AM-LJANG: Table 3), attributes in which *Osteoglossum* tends to differ from *Notopterus*.

Separate multivariate analyses of variance on the principal component scores for each behavior (raking and open-mouth chewing) reveal that the three species

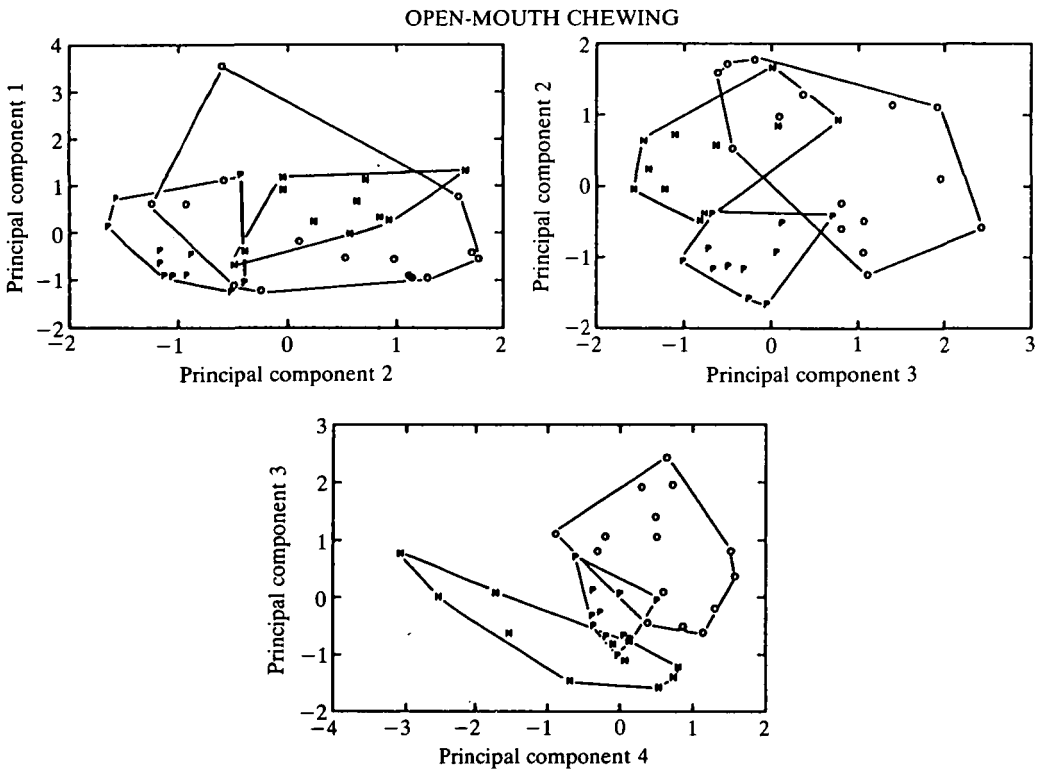

Fig. 11. Principal components (PC) analysis of open-mouth chewing behavior for eight kinematic variables plotted as PC1 *versus* PC2, PC2 *versus* PC3, and PC3 *versus* PC4. Principal components 1–4 account for the following percentages of the overall variance in the data set: PC1, 44.2 %; PC2, 23.7 %; PC3, 14.2 %; PC4, 11.1 %. These plots show that open-mouth chewing behavior in the three taxa studied (O, *Osteoglossum*; P, *Pantodon*; N, *Notopterus*) is kinematically similar for the first principal component (there are no significant differences among the centroids of the three species polygons; $P=1.38$, df 2, 34). However, the three species do show significantly different kinematics along principal components 2, 3 and 4 (MANOVA $P<0.001$).

are significantly different from each other in chewing kinematics for both behaviors even when all kinematic variables are considered together (raking: Wilks' Lambda $F=51.1$, df=8, 60, $P<0.0001$; open-mouth chewing: Wilks' Lambda $F=14.2$, df=8, 62, $P<0.0001$).

Discussion

There are two distinct behaviors that involve the TBA and can be identified in all three osteoglossomorph species studied: raking and open-mouth chewing. Both have distinctive kinematic patterns among the three taxa studied (Figs 10, 11): each species has a different method of using the TBA during raking and open-

Table 3. *Table of the principal component loadings of eight kinematic variables (described in the text)*

	Raking				Open-mouth chewing			
	1	2	3	4	1	2	3	4
AM-NELE	0.769	−0.328	0.039	0.358	0.208	0.392	0.741	0.474
AM-LJANG	0.689	−0.606	0.294	−0.122	0.149	0.713	−0.635	0.153
AM-PGDIS1	−0.084	0.895	−0.134	0.355	0.301	0.508	0.241	−0.745
AM-GAPE	0.342	0.556	0.668	−0.213	0.245	0.910	0.081	0.070
TM-NELE	0.561	0.556	−0.168	−0.435	0.922	−0.265	0.045	0.088
TM-LJANG	0.851	0.281	−0.083	0.175	0.820	0.048	−0.310	0.223
TM-PGDIS1	0.670	−0.089	−0.562	−0.244	0.944	−0.162	0.127	−0.142
TM-GAPE	0.853	0.073	0.080	0.199	0.951	−0.216	−0.062	−0.047

Four principal components (1–4) are listed for each of the two major intraoral prey-processing behaviors: raking and open-mouth chewing.

Raking and open-mouth chewing analyses were performed separately.

mouth chewing behaviors. Some overlap in kinematic pattern occurs in open-mouth chewing along principal component 1, but each species does possess some unique attributes (Fig. 11) and the overall MANOVA test of kinematic differences among species during open-mouth chewing is highly significant. Both raking and open-mouth chewing contribute significantly to prey destruction and disarticulation observed prior to swallowing.

Raking in *Osteoglossum* involves large excursions in neurocranial elevation, significantly greater than that found in either *Pantodon* or *Notopterus* (Table 1). The significant change seen in lower jaw angle is due to neurocranial elevation, as there is almost no change in gape, a feature common to all three taxa. Indeed, the key identifying feature of raking behavior is the nearly complete lack of change in gape as the prey is subjected to shearing and crushing forces by the TBA. The pectoral girdle in both *Osteoglossum* and *Pantodon* undergoes little change in position in comparison to *Notopterus* (Table 1). Thus, most of the power for raking comes from neurocranial elevation in *Osteoglossum* and *Pantodon*. We propose that during raking in *Osteoglossum* the mandibular jaw apparatus closes around the prey, stabilizing it. The basihyal teeth of the TBA are held in a fixed position (as little movement is visible in the hyoid and pectoral girdle regions) while the teeth on the ventral surface of the neurocranium and hyopalatine region are moved anterodorsally across the prey. The result of this behavior is extensive damage to the body wall and internal systems of the prey, as is evident from an examination of prey that are subsequently rejected and not swallowed.

Raking in *Pantodon* is a much quicker behavior, occurring on average in about half the time taken in *Osteoglossum* and *Notopterus* (Table 1). In common with *Osteoglossum*, the power stroke of the rake in *Pantodon* is characterized by a sharp decrease in neurocranial angle. While the neurocranium is rotating dorsally the jaws are being held closed and there is little change in gape distance. In

common with *Notopterus*, *Pantodon* begins to release its hold on the prey slightly prior to maximal neurocranial elevation. The reason for this is as yet unclear. As with *Osteoglossum* there is only a small change in the pectoral girdle distance. The pectoral girdle is held in position and the neurocranium is elevated, producing a shearing action between the neurocranium and the basihyal teeth, most of the power being generated by the neurocranium rotating dorsally.

As with the other two taxa, raking in *Notopterus* involves little change in gape distance and any change in neurocranial angle will be reflected by a similar change in lower jaw angle. The only exception to this is *Notopterus*, where the change in lower jaw angle is much smaller than the change in neurocranial elevation. This, however, could be accounted for by the slight increase in gape prior to maximal neurocranial elevation. The unique feature of raking in *Notopterus* is the large posterior movement of the pectoral girdle, which clearly acts to pull the hyoid apparatus and basihyal teeth (which have already penetrated the prey) through the prey item, thereby disarticulating and disemboweling it, and perhaps facilitating subsequent digestion. As the pectoral girdle moves posteriorly there is an increase in neurocranial angle (decrease in NELE). Electromyographic data confirming activity in the muscles retracting the pectoral girdle during raking behavior have been presented by Sanford and Lauder (1989).

Biomechanically, the raking mechanism in *Osteoglossum* and *Pantodon* appears to involve primarily anterodorsal movement of the skull and palatal teeth across the prey while the ventral teeth of the tongue bite appear primarily to stabilize the prey and hold it in position.

Open-mouth chewing in *Osteoglossum* is a very rapid behavior compared to raking. It occurs with the prey item located within the buccal cavity and involves substantial changes in gape distance. The significant increases in gape distinguish open-mouth chewing behavior from raking in all three species. *Osteoglossum* shows significantly greater excursions of the neurocranium than either *Pantodon* or *Notopterus*. In *Osteoglossum* the increase in neurocranial elevation contributes significantly to the increase in the gape. This is in contrast to both *Pantodon* and *Notopterus*, where the change in gape is almost entirely due to lower jaw depression. Open-mouth chewing begins with significant opening of the jaws caused by both neurocranial elevation and lower jaw depression and, at the same time, a slight posterior motion of the pectoral girdle. This is followed by closure of the mouth resulting from the raising of the lower jaw and an increase in geniohyoideus depression. It is clear that in *Osteoglossum* and *Pantodon* the use of the TBA during open-mouth chewing is not nearly as vigorous as it is in raking, and most of the action of the TBA results from neurocranial elevation. Open-mouth chewing in *Pantodon* is slightly different from that in *Osteoglossum* as there is not nearly as much neurocranial elevation. One of the most characteristic features of open-mouth chewing in *Notopterus* is the significantly smaller change in gape when compared to the other taxa. *Notopterus* typically opens its mouth about 13% of head length in contrast to values of nearly 30% in *Pantodon* and *Osteoglossum*.

One issue that might complicate interpretations of comparative kinematic patterns is the difference in prey types used: *Notopterus* was fed live fish while *Pantodon* and *Osteoglossum* were fed crickets on the surface of the water. This mimics the natural prey chosen by these fishes, but opens the possibility that the kinematic attributes of *Notopterus* that differ from those of *Pantodon* and *Osteoglossum* might be due only to prey type. Indeed, the large posterior excursions of the pectoral girdle may function primarily to disable live potentially evasive prey. However, many other aspects of TBA kinematics differ between *Pantodon* and *Osteoglossum*, indicating that even large kinematic differences may be found when prey types are identical. In addition, *Notopterus* shares many features of TBA kinematics with both *Pantodon* (e.g. the amount of neurocranial elevation during raking) and *Osteoglossum* (e.g. long duration to peak neurocranial elevation during raking behavior), indicating that the type of prey eaten does not allow prediction of TBA kinematics.

A second issue that could theoretically complicate our comparative analysis is the difference in size of the three species. The variables that are most obviously affected by size differences are the raw distance measurements. One way of attempting to correct for size differences is to consider the amplitude of the jaw movements as a percentage of head size (although this correction will not be completely effective if variables scale allometrically). We have used these values (given in Table 1) as a guide to interpreting interspecific kinematic patterns and in formulating the description of kinematic events. In addition, we note that kinematic variable means do not sort according to species size. For example, the smallest species (*Pantodon*) has kinematic durations that are both longer and shorter than those of the larger species, as well as amplitude variables that are both larger and smaller than those of the larger species (Table 1). Similarly, the largest species (*Notopterus*) has some variables for which the values are smaller than in *Osteoglossum* and *Pantodon*. Simple differences in size are thus unable to account for the major differences in kinematic pattern that we have found in these three species.

The major conclusion of this kinematic analysis is that the kinematic patterns used by the three species of osteoglossomorph fishes studied are significantly different from each other during both chewing behaviors. Possession of a similarly specialized morphological system (the TBA) does not imply kinematic similarity. Each of the three species appears to have divergent kinematic patterns for utilizing a similar morphological specialization. This result suggests that fruitful avenues of future research will be detailed comparative investigations of both the morphology of the TBA and the muscle activity patterns producing chewing behaviors.

We thank Peter Wainwright, Steve Reilly and Miriam Ashley for invaluable comments on the manuscript, and Heidi Mumford for excellent laboratory assistance as well as aid in digitizing. This research was supported by a NATO/NERC grant GT8/F/87/ALS/1 to CPJS and NSF grants BSR 85–20305, DCB 8710210 and BBS 8820664 to GVL.

References

BRIDGE, T. W. (1895). On certain features of the skull of *Osteoglossum formosum*. *Proc. zool. Soc., Lond.* **20**, 302–310.

DAGOT, J. AND D'AUBENTON, F. (1957). Development et morphologie de crane d'*Heterotis niloticus* Ehrenberg. *Bull. Inst. Fr. Afr. noire* (A) **19**, 881–936.

D'AUBENTON, F. (1954). Etude de l'appareil branchiospinal et de l'organe suprabranchia d'*Heterotis niloticus* Ehrenberg 1927. *Bull. Inst. Fr. Afr. noire* (A) **17**, 1179–1201.

DINGERKUS, G. AND UHLER, L. D. (1977). Enzyme clearing of alcian blue stained whole small vertebrates for demonstration of cartilage. *Stain Tech.* **52**, 229–232.

GREENWOOD, P. H. (1970). On the genus *Lycoptera* and its relationships with the family Hiodontidae (Pisces, Osteoglossomorpha). *Bull. Br. Mus. nat. Hist. Zool.* **19**, 257–285.

GREENWOOD, P. H. (1971). Hyoid and ventral gill arch musculature in osteoglossomorph fishes. *Bull. Brit. Mus. nat. Hist. Zool.* **22**, 1–55.

GREENWOOD, P. H. (1973). Interrelationships of osteoglossomorphs. In *Interrelationships of Fishes* (ed. P. H. Greenwood, R. S. Miles and C. Patterson), pp. 307–332. New York: Academic Press.

KERSHAW, D. (1970). The cranial osteology of the 'butterfly fish' *Pantodon buchholzi*. *Zool. J. Linn. Soc., Lond.* **49**, 5–19.

KERSHAW, D. (1976). A structural and functional interpretation of the cranial anatomy in relation to the feeding of osteoglossoid fishes and a consideration of their phylogeny. *Trans. zool. Soc., Lond.* **33**, 173–252.

LAUDER, G. V. (1980). Evolution of the feeding mechanism in primitive actinopterygian fishes: a functional anatomical analysis of *Polypterus*, *Lepisosteus*, and *Amia*. *J. Morph.* **163**, 283–317.

LAUDER, G. V. AND LIEM, K. F. (1983). The evolution and interrelationships of the actinopterygian fishes. *Bull. Mus. comp. Zool.* **150**, 95–197.

LIEM, K. F. AND GREENWOOD, P. H. (1981). A functional approach to the phylogeny of the pharyngognath teleosts. *Am. Zool.* **21**, 83–101.

NELSON, G. J. (1968). Gill arches of some teleostean fishes of the division Osteoglossomorpha. *Zool. J. Linn. Soc., Lond.* **47**, 261–277.

NELSON, G. J. (1969*a*). Infraorbital bones and their bearing on the phylogeny and geography of osteoglossomorph fishes. *Am. Mus. Novit.* **2394**, 1–37.

NELSON, G. J. (1969*b*). Gill arches and the phylogeny of fishes, with notes on the classification of vertebrates. *Bull. Am. Mus. nat. Hist.* **141**, 475–552.

OMARKHAN, M. (1950). The development of the chondrocranium of *Notopterus*. *Zool. J. Linn. Soc., Lond.* **61**, 608–624.

RIDEWOOD, W. G. (1904). On the cranial osteology of the families Mormyridae, Notopteridae, and Hyodontidae. *J. Linn. Soc.* **29**, 188–217.

RIDEWOOD, W. G. (1905). On the cranial osteology of the fishes of the families Osteoglossidae, Pantodontidae and Phractolaemidae. *J. Linn. Soc.* **29**, 252–282.

SANFORD, C. P. J. AND LAUDER, G. V. (1989). The functional morphology of the 'tongue-bite' in the osteoglossomorph fish *Notopterus*. *J. Morph.* **202**, 379–408.

TAVERNE, L. (1977). Osteologie, phylogenese et systematique des teleosteens fossiles et actuels du super-ordre des Osteoglossomorphes. Premiere partie. Osteologie des genres *Hiodon, Eohiodon, Lycoptera, Osteoglossum, Scleropages, Heterotis* et *Arapaima*. *Acad. R. Belg. Mem. Cl. Sci., Coll.* in-8°, 2^{e} ser., T.XLII, F.3, 235pp.

TAVERNE, L. (1978). Osteologie, phylogenese et systematique des Teleosteens fossiles et actuels du super-ordre des Osteoglossomorphes. Deuxieme partie. Osteologie des genres *Phareodus, Phareoides, Brychaetus, Musperia, Pantodon, Singida, Notopterus, Xenomystus* et *Papyrocranus*. *Acad. Roy. Belg., Mem. Cl. Sc., Coll.* in-8^{0}, 2^{e} ser., T.XLII, F.6, 213pp.

WINTERBOTTOM, R. (1974). A descriptive synonymy of the striated muscles of the Teleostei. *Proc. natn. Acad. Sci. (Phil.)* **125**, 225–317.